

Safety of the Package of Natural UF₆ Under Fire Conditions*

M. Wataru, A. Kosaki, O. Kato
Central Research Institute of Electric Power Industry

H. Fujiwara
Ishikawajima-Harima Heavy Industries Co., Ltd.

J. Nobe
Mitsubishi Research Institute, Inc.

INTRODUCTION

In the IAEA's Transport Regulations of 1996, it is planned that a thermal test requirement is imposed on packages shipping natural uranium hexafluoride (UF₆) taking account of chemical hazard in addition to the radiological hazard. However, it is very difficult to evaluate the safety of the packages under fire conditions because the thermal behavior of UF₆ is very complicated. Several studies have been performed on the thermal behavior of UF₆ in the packaging (Yamakawa et al. 1988), most of which have been analytical studies because UF₆ is difficult to use in tests. Compared with their results, it is impossible to say that thermal behavior of UF₆ in the packaging has been already made clear. The main characteristic of the thermal behavior of UF₆ is its low temperature triple point, phase change, and volume expansion, and it is difficult to get an accurate solution for a calculation taking account of all of them. To provide an accurate solution, it is necessary to assess the thermal phenomena of UF₆ in the packaging by experimental studies, yet there are few existing experimental studies with UF₆. Although interesting results have been obtained, they are not enough to make a calculation model. To assess the thermal behavior of UF₆ in the packaging of natural UF₆, an experimental study called a TENERIFE project has been in progress. In the study, tests are carried out using a container with full scale diameter but shorter length containing real UF₆. To evaluate the safety of the package of natural UF₆ under fire conditions, mechanical analysis of the package and measurement of UF₆ leakage from the valve are needed.

MATERIAL PROPERTIES OF THE PACKAGING AT HIGH TEMPERATURE

ASME SA 516 carbon steel for moderate and lower temperature service is currently used as the structural material for natural UF₆ packagings. When the natural UF₆ package is involved in a fire, the inner pressure increases depend on the UF₆ gas pressure. The structural strength of the packaging decreases with increasing temperature, so the

* This work was conducted under a contract from the Science and Technology Agency of Japan.

possibility of rupture of the packaging should be studied (Kosaki et al. 1994). As SA 516 steel is not generally used for high temperature work, tensile and creep data are not available above 500°C.

High Temperature Tensile Tests

Tensile tests from room temperature up to 900°C were conducted using several base metal and seam-welded joints of SA 516 produced in the U.S.A., France, and Japan. The strain rate in the high temperature tensile tests was $5 \times 10^{-3} \text{ min}^{-1}$ and over 0.2% proof stress was $6 \times 10^{-2} \text{ min}^{-1}$. An example of the results is shown in Figure 1. The tensile strength values and 0.2% proof stress decrease with increasing temperature. No influence of phase transformation was observed. On the other hand, the values of the reduction area and elongation increase with increasing temperature. The position of rupture of seam-welded joints was the base metal at temperatures from room temperature up to 800°C, but at 900°C, the rupture position was the weld metal.

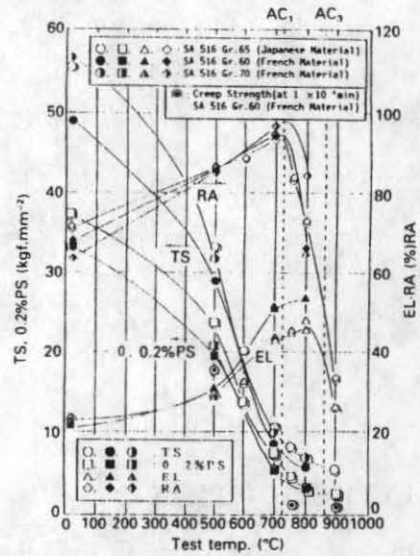


Fig.1. Results of Tensile Tests at High Temperature

Creep Deformation Properties under Fire Conditions

According to the results of preliminary creep tests, creep-rupture strength is smaller than tensile strength and it is clear that the strength depends on the strain rate. Assessment by creep strength thus gives a more conservative estimate than by tensile strength, so creep deformation data were obtained by uniaxial creep tests, internal pressure creep tests, and internal pressure creep rupture tests.

Short-time uniaxial creep tests were conducted at 600° to 900°C(600,700,750, 800, 900) and at three different stress levels (0.8 to 4.5kgf · mm⁻²) at each temperature using SA 516 Gr.65 base metal and its seam-welded joints. The test results show that in the temperature range of 600° to 800°C, the creep deformation at the heat-affected zone is larger than the deformation of the base metal or weld-metal. From these test results, creep deformation formula which represent the secondary creep region were obtained.

$$\epsilon_c = (\epsilon_\tau + \epsilon_s \cdot t) \quad (1)$$

$$\epsilon_\tau = \epsilon_\tau^s \{1 - \exp(-1.723(\epsilon_s \cdot t)^{0.528})\} \quad (2)$$

$$\epsilon_\tau^s = \exp(0.581 \sigma) \exp\left(-\frac{5.06 \times 10^3}{T+273} + 1.21\right) \quad (3)$$

$$\epsilon_s = \exp(1.471 \sigma) \exp\left\{-\frac{1.03 \times 10^8}{(T+273)^2} + \frac{1.76 \times 10^5}{(T+273)} - 77.3\right\} \quad (4)$$

where,

ϵ_c : creep strain(%) ϵ_τ : creep strain of transition creep(%)

ϵ_τ^s : saturated transition creep strain(%) ϵ_s : minimum creep rate(% · h⁻¹)

t: time(h) σ : creep stress(kgf · mm⁻²) T: test temperature(°C)

To evaluate the creep deformation from the internal pressure, creep tests were conducted by using cylindrical test pieces of SA 516 Gr.65 base metal (Fig.2). The test temperature was 700°, 750° and 800°C, and the circumference stress applied by internal gas pressure was 3.0 and 1.5kgf · mm⁻² at each temperature. The results of the internal pressure creep showed that the creep deformation equation obtained by the uniaxial creep tests is applicable. Circumferential creep deformation was determined by measuring the outer diameter of test pieces intermittently during the tests and the final thickness of the test pieces was measured after the tests. To estimate the deformation from internal pressure, a simple creep deformation formula using Norton's law was obtained for the secondary creep region. According to Norton's law, the circumferential strain rate for internal pressure creep tests can be expressed as follows;

$$\dot{\epsilon}_{\theta} = 3^{n+1/2} \cdot \frac{K}{2} \cdot \left(\frac{P \cdot a}{2t} \right)^n \quad (5)$$

$$K = 0.0107(\text{at } 700^{\circ}\text{C}), 0.0478(\text{at } 750^{\circ}\text{C}), 0.1190(\text{at } 800^{\circ}\text{C})$$

$$n = 3.93$$

where,

a: radius of cylinder (mm)

P: internal pressure (kgf · mm⁻²)

t: thickness of cylinder (mm)

$\dot{\epsilon}_{\theta}$: circumferential strain (% · h⁻¹)

The test results at 700°C and 750°C show good agreement with the test results and estimated values but, at 800°C, the test results were a little lower than the estimated values, because Norton's law ignores preliminary creep strain. Using the test pieces of base metal and seam-welded joints in the same configuration as shown in Figure 2, internal pressure creep rupture tests were conducted at 600°, 700°, 750°, and 800°C. Figure 3 shows the relation between the stress in the circumferential direction, test temperature, and time to rupture. From these results, circumferential life-time formula for internal pressure creep rupture were obtained as follows:

$$\sigma = F(T) \times t_r^{-G(T)} \quad (6)$$

$$F(T) = -1.42(T/100)^3 + 33.15(T/100)^2 + 259.11(T/100) + 682.34 \quad (7)$$

$$G(T) = -0.04967(T/100)^3 + 1.0915(T/100)^2 - 7.902(T/100) + 19.010 \quad (8)$$

(600°C < T < 800°C)

where,

σ : stress in the circumferential direction (kgf · mm⁻²) t_r : time to rupture (h)

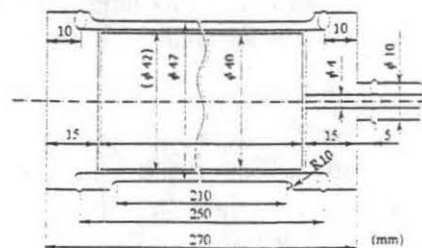


Fig.2. Test Piece for Inner Pressure Test

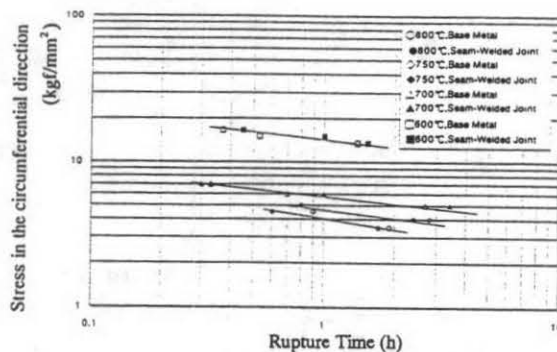


Fig.3. Relation between the Stress in the Circumferential Direction, Test Temperature, and Rupture Time

Creep Deformation Properties under Variable Conditions

When the package is in a fire accident, the temperature of the packaging and internal pressure change over time, so it is necessary to estimate the creep deformation and the circumferential life-time under transient conditions. Short-time uniaxial creep tests were conducted under variable temperature or variable stress using SA 516 Gr.65 base metal. In the variable stress tests, the stress changed from 1.5 to 3.0 or 3.0 to 4.5 $\text{kgf} \cdot \text{mm}^{-2}$ at constant temperature (700° or 800°C), while in the variable temperature tests, the temperature changed from 700° to 750° or 750° to 800°C at constant stress (1.5 or 4.5 $\text{kgf} \cdot \text{mm}^{-2}$). For a conservative estimate, the ratio of the experimental value to the estimated value at 5% strain, which is the threshold between the secondary creep and third creep region, was calculated from the test results. As a result, the following coefficients were obtained, for the conservative estimation of strain.

$$\alpha = (\text{experiment value})/(\text{estimated value}) \quad (9)$$

$\alpha = 1.2$ at constant temperature and stress

1.5 at variable temperature and stress at lower than 700°C

1.8 at variable temperature and stress at higher than 800°C

Strain can thus be estimated at variable temperature and stress by using these coefficients.

On the circumferential life-time, internal pressure creep rupture tests at variable temperature and stress were conducted using SA 516 Gr.65 base metal and seam-welded joints. According to Robinson's law, in case of changing temperature and stress, the rupture is assumed to occur when the sum of the creep damage factor is equal to 1. The creep damage factor is calculated by the following formula using time to rupture calculated by formula (6) ~ (8).

$$D = \sum (t_i / t_{ri}) \quad (10)$$

where,

D: creep damage factor t_i : time at certain constant condition

t_{ri} : time to rupture calculated by formula (6) ~ (8)

In case of the variable temperature tests, the temperature changes from 700° to 750° or 750° to 800°C at constant stress (5.5 or 4.5 $\text{kgf} \cdot \text{mm}^{-2}$). In case of the variable stress tests, the stress changes from 5.0 to 6.0, 6.0 to 7.0, 13.5 to 15.0, or 15.0 to 16.0 $\text{kgf} \cdot \text{mm}^{-2}$ at constant temperature (700° or 600°C). Calculating the creep damage factor using the test data, the values range from 0.6 to 1.5 because of the scatter in measurements. For the conservative estimation of time to rupture, the creep damage factor should be smaller than 0.6.

MEASUREMENT TESTS OF THE LEAKAGE FROM A VALVE

The packaging of natural UF_6 has a 1-inch valve and plug. At these parts, there is no UF_6 leakage under normal conditions. But, if the bare packaging is in a fire accident, UF_6 could leak from the valve and plug. The valve and plug with solder are screwed in the coupling of the packaging. Leakage may occur at the screw parts because the solder melts at 200°C, and also at the stem part of the valve because Teflon packings lose their leaktightness at high temperature. To estimate the amount of UF_6 leakage under fire conditions, measurement tests of leakage from the valve were conducted using an actual 1-

inch valve and nitrogen gas at high temperature (up to 600°C) and internal pressure (up to 30kgf · cm⁻²). Figure 4 shows the test equipment and Figure 5 shows the test specimen. The test specimen is connected to the pressurizing loop and put in the chamber equipped with an electrical heater. To avoid the temperature of the test specimen falling due to leakage gas, pressurizing gas is also heated. At constant temperature and pressure, leakage rates were measured. The leakage rates were estimated approximately from the pressure difference and leakage conductance.

From the tests results, the leakage conductance was obtained as follows:

$$L = F(T)\{P_u - P_d\} \quad (11)$$

$$F(T) = 2.43 \times 10^{-5} \times T - 7.13 \times 10^{-3} \quad (12)$$

where,

L: leakage rate (m³ · sec⁻¹)

F(T): leakage conductance
(m³ · sec⁻¹ · bar⁻¹)

T: temperature (°C)

P_u: upstream pressure (bar)

P_d: downstream pressure (bar)

Formula (12) was obtained from the test data under constant conditions. To verify the applicability of this formula under transient conditions, leakage measurement tests were conducted, in which the temperature and/or pressure was changed. Temperature was changed from room temperature to 600°C and pressure from 1 to 25 bar (Fig. 6). The estimated values agreed approximately with the test result so it is clear that the formula (12) can be used under transient conditions (Fig. 7).

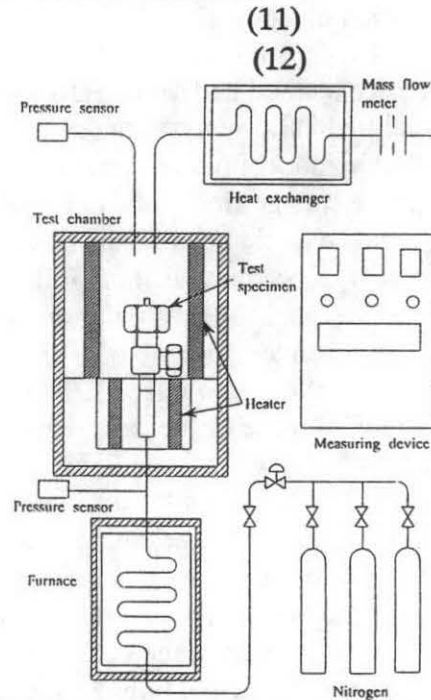


Fig. 4. Outline of the Leakage Tests Equipment

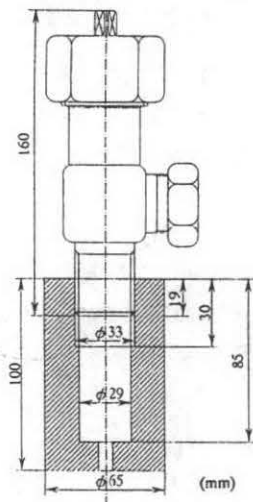


Fig.5. Specimen of Valve Test

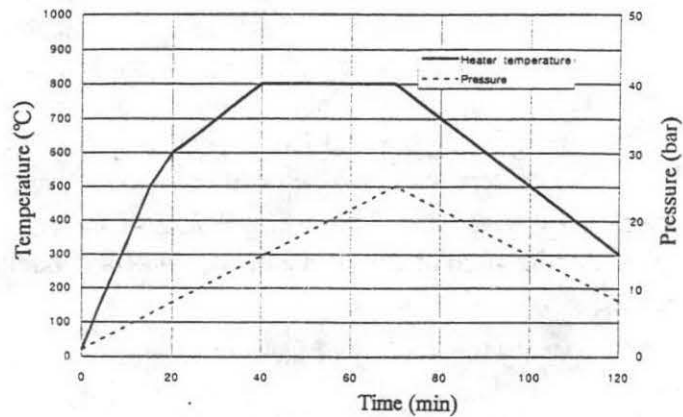


Fig.6. Test Conditions of Leakage Test

THERMAL ANALYSIS METHOD

When UF_6 is heated up from room temperature, it changes from solid to liquid and vapor. During the melting process, solid UF_6 sinks in the liquid UF_6 and liquid UF_6 moves by natural convection. After all the UF_6 melts, the liquid level increases slowly because of the volume expansion of UF_6 . Taking account of these phenomena, the thermal calculation model was developed using FLUENT code. FLUENT code is based on the finite difference method and Transient Flow Rate on thermal hydraulic analysis can be made. The calculation model involves several assumptions.

The phase change from solid to liquid is taken into account by the enthalpy method. While a solid and a liquid coexist, the Navier-Stokes equation is solved in both the solid and liquid region assuming that the solid region is a liquid which has a very high viscosity, about a thousand times as much as that of the liquid. When the phase changes from solid to liquid and then temperature of UF_6 increases, the volume of UF_6 increases, because UF_6 has volume expansion rate. If UF_6 level goes up, it influences the inner pressure and the temperature profile of the packaging. The temperature profile of the packaging is also important to make a structural analysis. To simulate the volume expansion of UF_6 , the grid size was changed when the total volume increased with temperature by 5%. The initial volume of UF_6 in the packaging was 60% and then it was changed to 65, 70, 75, 80, 85, 90, 95, 100% (Fig. 8). The grid is made as a body-fitted coordinate, and only the grids which are higher than the center level are changed to simplify the model. When the grid size changes, it is assumed that the temperature, energy, and velocity of the new grids are equal to those of the old one. In this case, because of the discontinuous volume expansion, the energy balance is not conserved, so the equivalent specific heat is used to satisfy the energy balance depending on the grid size and temperature. The temperature dependence of density, viscosity, and thermal conductivity are taken into account.

Boundary Condition

The packaging is heated up by only radiation from ambient at 800°C . The emissivities of the surroundings and the outer surface of the packaging are 0.9 and 0.6 respectively. The initial volume of UF_6 (solid) in the packaging is 60%. In the upper part of the packaging, radiation heat flux is taken into account but not convection. The emissivities of the inner surface and UF_6 are 0.8 and 1.0 respectively. The shape factor between the packaging and UF_6 changes depending on the position of UF_6 level. In UF_6 , thermal hydraulic calculations were carried out using FLUENT code. To evaluate the turbulent flow, the $k-\epsilon$ model was used. The boundary condition of the inner surface is no-slip.

Results

First, to verify the validity of the modeling, some experiments were performed using a substitute material for UF_6 , C_6F_{12} (Table 1). C_6F_{12} is solid at room temperature and has triple point at low temperature. It is white as a solid and transparent as a liquid. The dimension of the test container made of stainless steel is about 100 mm diameter \times 150 mm

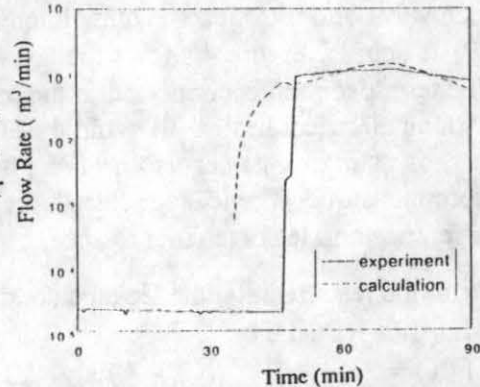


Fig. 7. Comparison between Test Data and Calculation Data

length. On the both sides, there is glass to allow the thermal behavior to be watched during the tests. The test container is heated under vacuum so that it receives heat by radiation only (Fig. 9). The heater temperature is 350°C and filling rate is 50% of the container. After the calibration test using an empty container to determine the heat flux from the heater to the container, some experiments were performed. The calculation results agreed well with the test results (Fig. 10). The model does not involve thermal gap between the inner surface of the container and solid UF₆ because of sublimation. At the first stage of heating, the temperature of the container is different between the test result and calculation result because of the thermal gap (thermal gap effect), but after liquid C₆F₁₂ wets the inner surface, the two data agree well, and the inner pressure agrees well, too. These test results show that the inner pressure depends on the free surface temperature.

Second, using this model, the calculation result was compared with the test result of the TENERIFE program, which is developed in a joint program between France and Japan. In this program, a test container of full-scale diameter and 1/3 length containing UF₆ is used. Comparing the calculation result with the test result for 18 min heating at 800°C, the temperature of the container agrees well except for thermal gap effect (Fig. 11). This agreement shows the model can evaluate the UF₆ level. However, the temperature does not agree, especially near the free surface where the test data are larger than the calculation, so the inner pressure defined by the temperature of the free surface is also different. In this model, the natural convection effect may be bigger than the real phenomenon, thus preventing an increase of the local temperature.

CONCLUSION

The results obtained from several kinds of tests were as follows:

Tensile tests, uniaxial creep tests, internal pressure creep tests and internal pressure creep rupture tests were conducted at high temperature, and the material properties of a natural UF₆ package were obtained. These data are necessary to evaluate the structural analysis.

Using 1-inch valve leakage tests at high temperature and pressure with nitrogen, the empirical estimation formula of the leakage rate was proposed.

Heat transfer tests using a substitute material for UF₆ showed that the inner pressure depends on the free surface temperature.

A calculation model taking account of the phase change, natural convection, and sinking of solid and volume expansion was developed, and the results calculated by this model show that the temperature profile of the packaging and UF₆ level position agree with the test results, but that the UF₆ temperature profile and inner pressure are underestimated.

REFERENCES

- A.Kosaki, T.Ajima, H.Fujiwara, and M.Wataru: Material properties of a natural UF₆ transport cylinder vessel at high temperature, *Int. J. of Radioactive Materials Transport*, Vol.5, Nos2-4, 1994.
- H.Yamakawa and S.Shiomi: Safety evaluation of the transport container for natural UF₆ under the fire accident, UF₆ safe handling processing and transporting, CONF880558, Oak Ridge, Tennessee, 1988.

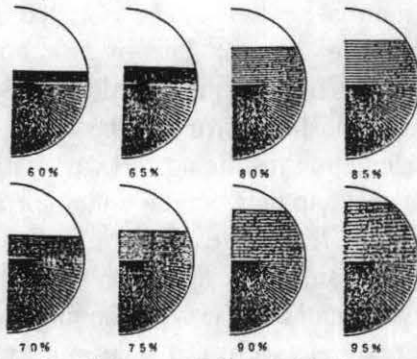


Fig. 8. Change of the Grid Size (UF6)

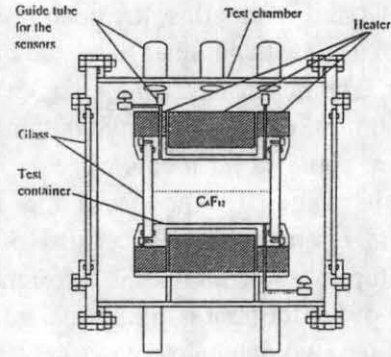
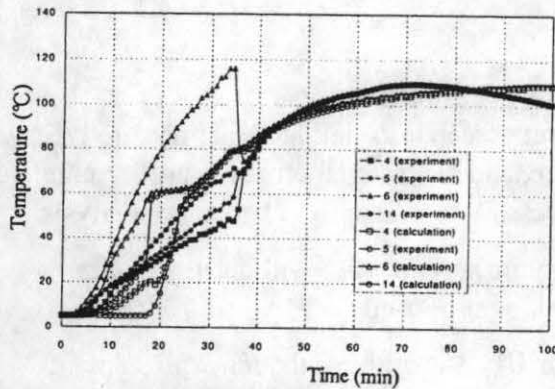
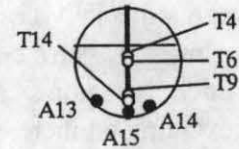
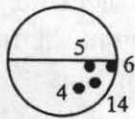


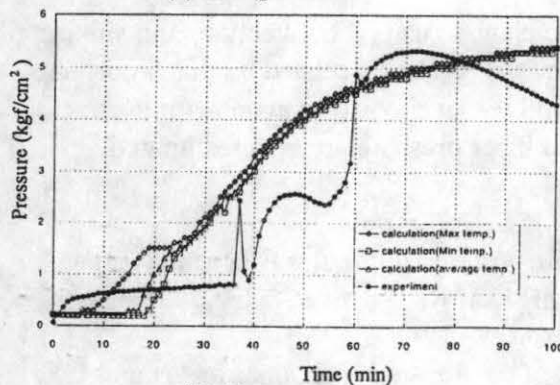
Fig. 9. Test Equipment of C6F12 Test

Table 1. Properties of UF6 and C6F12

Item	UF ₆	C ₆ F ₁₂
Specific Heat : cal/(g · °C)	Solid(50°C) 0.1195	Solid(30°C) 0.2457
	Liquid(64~150°C) 0.133	Liquid(80°C) 0.3177
Latent Heat : cal/g	12.95	3.97
Heat of Sublimation : cal/g	32.33	28.1
Heat of Vaporization : cal/g	19.49	23.0
Volume expansion rate : °C ⁻¹	64~150°C : 1.38 × 10 ⁻²	60~65°C : 2.9 × 10 ⁻²
Heat Conductivity : W/(m · K)	50°C : 0.0473	30°C : 0.088
	72°C : 0.160	52°C : 0.175
Viscosity : mPa · s	9.1 × 10 ⁻¹	8.14 × 10 ⁻¹
Triple Point	64.1°C, 1.5kgf/cm ²	62.5°C, 1.55kgf/cm ²
Sublimation	56.6°C, 1.03kgf/cm ²	52.8°C, 1.03kgf/cm ²
Density : g/cm ³	5.09(20°C)	1.9(20°C)
	3.65(64°C)	

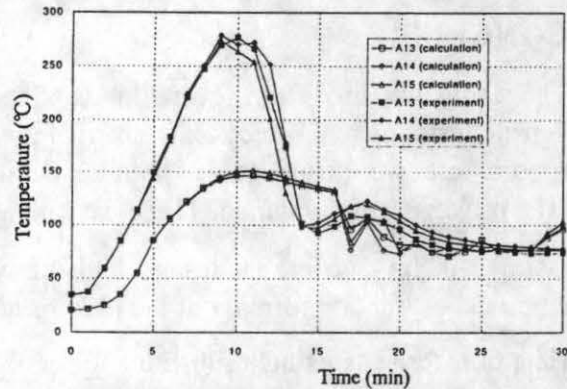


(a) Temperature

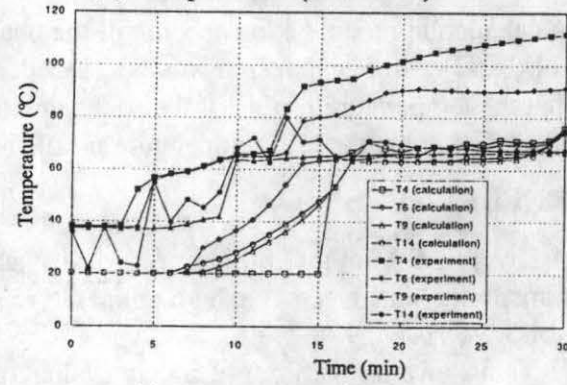


(b) Pressure

Fig. 10. Comparison between Test Data and Calculation Data (C6F12)



(a) Temperature (container)



(b) Temperature (UF6)

Fig. 11. Comparison between Test Data and Calculation Data (UF6)